Electronic Supplementary Material (ESI) for Dalton Transactions.

Supporting Information

Large-Scale Synthesis, Mechanism, and Application of a Luminescent Copper Hydride Nanocluster

Tingting Xu,[‡a] Endong Wang,[‡c] Shuai Liu,[a] Zhezhen Wei,[a] Peiqun Yin,[d] Jianan Sun,[d] Wen Wu Xu[b*] and Yongbo Song[a,d*]

[a]School of Basic Medical Sciences, Anhui Medical University, Hefei, 230032, China.

[b]Department of Physics, School of Physical Science and Technology, Ningbo University, Ningbo 315211, China.

[c]School of Chemistry and Chemical Engineering, Liaoning Normal University, Dalian 116029, China.

[d]School of Biomedical Engineering, Anhui Medical University, Hefei, Anhui 230032, China.

Corresponding authors: xuwenwu@nbu.edu.cn; ybsong860@ahmu.edu.cn;

Large-scale synthesis of Cu_4H NCs.

The large-scale synthesis of the Cu_4H NCs was gradually amplified by 10-fold, 20-fold and 30-fold. Herein, the 30-fold synthesis method is discussed. 6 g disphenyl-2-pyrldylphosphine was added into 180 mL methanol solution of cuprous chloride (1.5g) with vigorously stirring (~1200 rpm) at room temperature. After string for 30 min, 3.6 g borane-tert-butylamine complex was added in the above solution. After 5 h, 10 mL methanol solution of sodium tetraphenylboron (0.15 g) was mixed with the reaction solution, which was centrifuged. And then, the yellowish precipitate was retained and washed with n-hexane/ethanol three times to remove the redundant ligands and by-products. Finally, ~5.86 g of pure Cu_4H NCs was obtained with a ~90% yield (Cu atom basis).

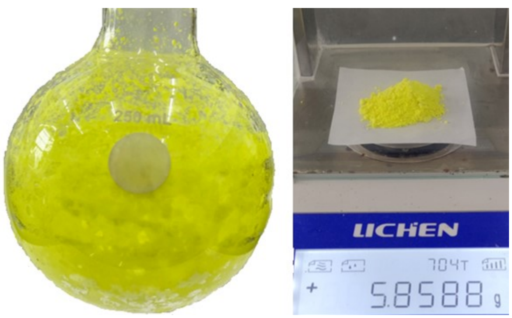

Fig. S1 The pictures of the production of 30-fold synthesis.

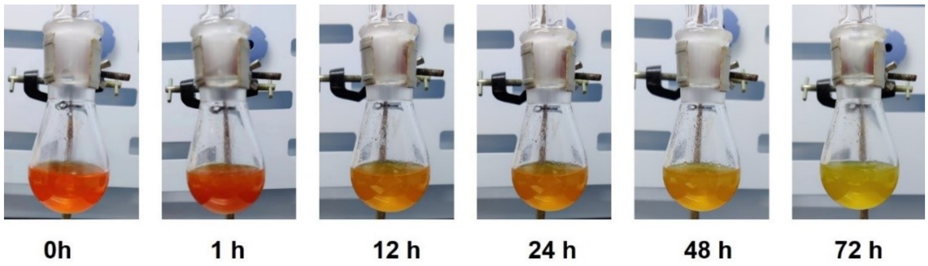

Fig. S2 Photographs of the reaction system using $NaBH_4$ at different times.

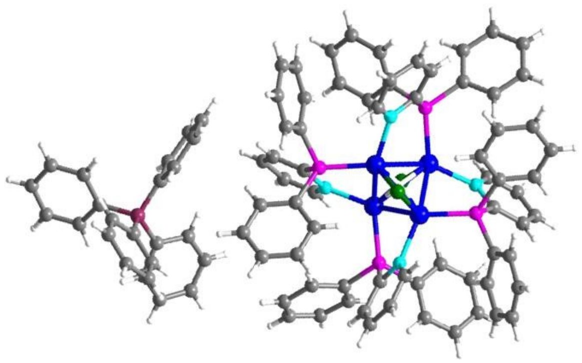

Fig. S3 Total structure of Cu_4H NC with the counterion of Ph_4B^-. Color labels: blue = Cu; green = Cl; magenta = P; light blue = N; grey = C; purple = B; white = H.

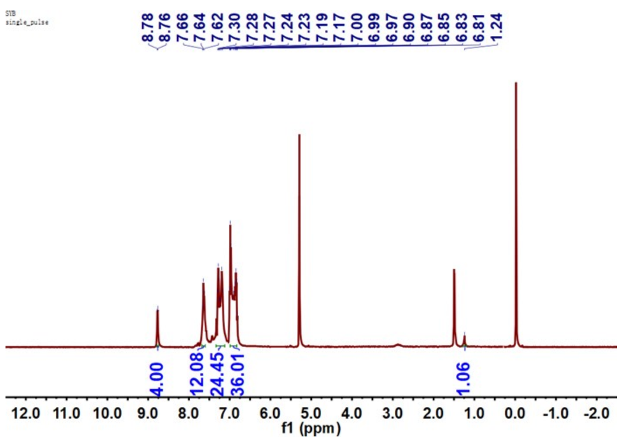

Fig. S4 The [1]H NMR spectrum of Cu_4H NCs dissolved in CD_2Cl_2 (note: the peak at 1.48 ppm can be assigned to protons from H_2O).

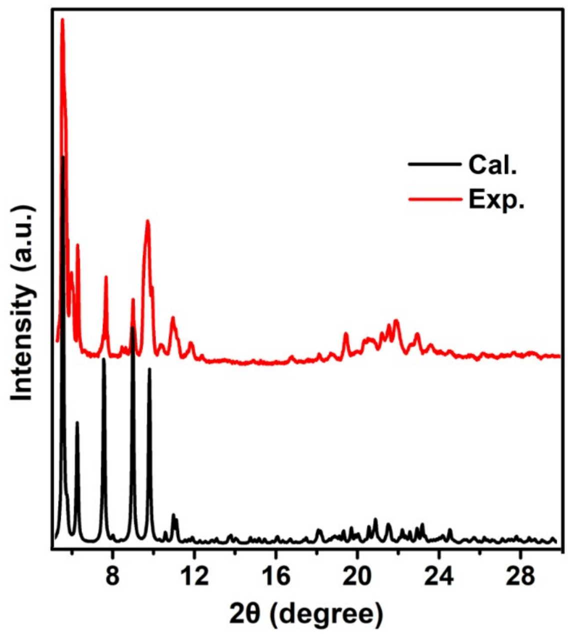

Fig. S5 The PXRD spectra of the Cu_4H NCs prepared in large-scale.

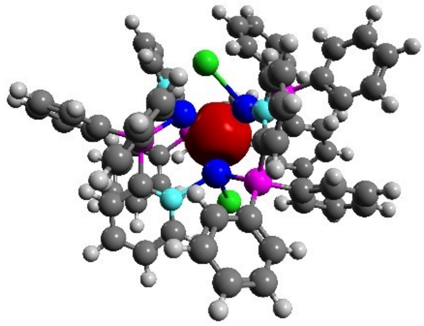

Fig. S6 Localized molecular orbital that reflects the valence electron population.

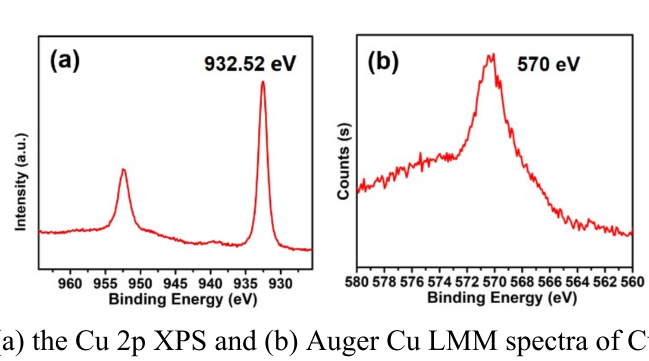

Fig. S7 (a) the Cu 2p XPS and (b) Auger Cu LMM spectra of Cu_4H NCs.

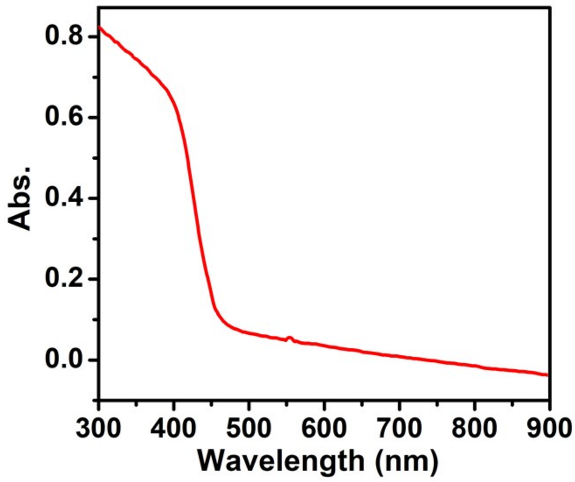

Fig. S8 The UV-vis absorption spectrum of Cu_4H NCs in solid state.

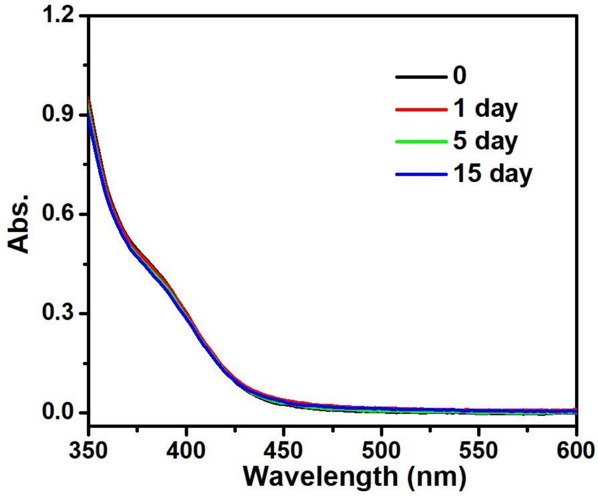

Fig. S9 Time-dependent UV-vis absorption spectra of Cu_4H NCs in dichloromethane.

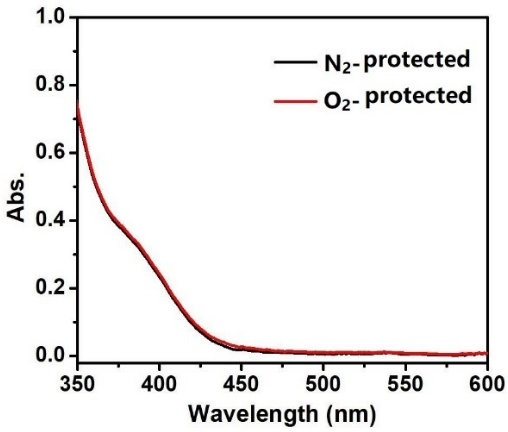

Fig. S10 The UV-vis spectra of Cu_4H NCs in the N_2-protected and O_2-protected CH_2Cl_2 solution.

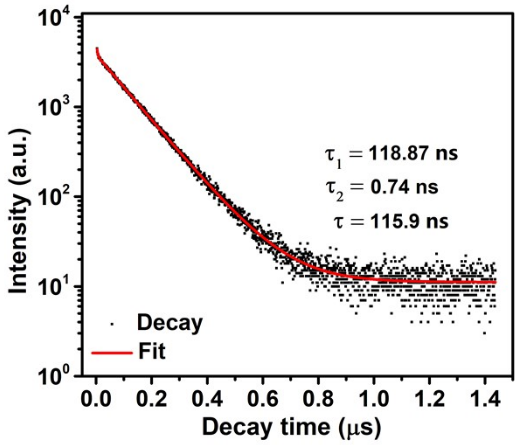

Fig. S11 Emission lifetime of Cu_4H NCs in the CH_2Cl_2 at air atmosphere.

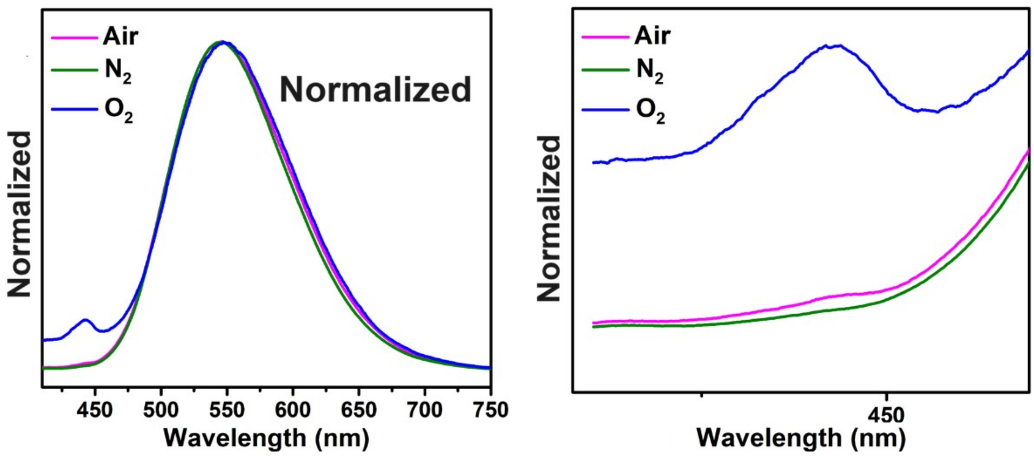

Fig. S12 The normalized emission spectra of Cu_4H NC in CH_2Cl_2 solution under O_2, air and N_2 atmospheres (left) and the corresponding magnified spectra (right).

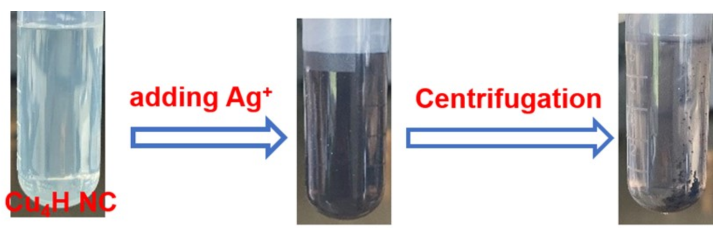

Fig. S13 Photographs of the reaction process of Cu_4H NCs with Ag^+ ions.

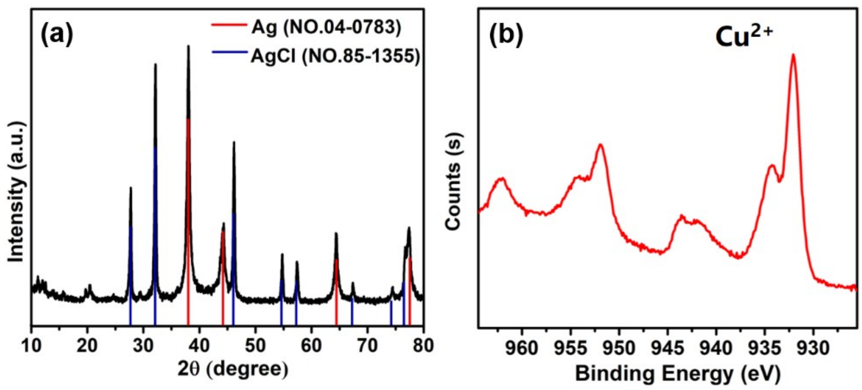

Fig. S14 (a) the PXRD spectrum of the precipitation; (b) the Cu 2p XPS spectrum of supernatant.

Table S1 Crystal data and structure refinement for Cu_4H.

Empirical formula	$C_{92}H_{77}BCl_2Cu_4N_4P_4$
Formula weight	1698.31
Temperature/K	120(2)
Crystal system	monoclinic
Space group	$P2_1/c$
a/Å	16.0437(3)
b/Å	30.6258(7)
c/Å	18.2015(4)
α/°	90
β/°	97.903(2)
γ/°	90
Volume/Å^3	8858.4(3)
Z	4
ρ_{calc}g/cm^3	1.273
μ/mm^{-1}	2.661
F(000)	3484.0
Crystal size/mm^3	0.1 × 0.08 × 0.06
Radiation	CuKα (λ = 1.54186)
2Θ range for data collection/°	8.418 to 124.988
Index ranges	$-16 \leq h \leq 18$, $-26 \leq k \leq 35$, $-17 \leq l \leq 20$
Reflections collected	34146
Independent reflections	13781 [R_{int} = 0.0399, R_{sigma} = 0.0517]
Data/restraints/parameters	13781/1080/968
Goodness-of-fit on F^2	0.799
Final R indexes [I>=2σ (I)]	R_1 = 0.0460, wR_2 = 0.1272
Final R indexes [all data]	R_1 = 0.0601, wR_2 = 0.1364
Largest diff. peak/hole / e Å^{-3}	0.74/-0.56

Table S2 Orbital populations for the HOMO and LUMO orbital of the S_0 state and S_1 state of the Cu_4H cluster calculated at the B3LYP/LANL2DZ level.

S_0 state of the Cu_4H cluster							
	Cu_sp	***Cu_d***	***Cl_sp***	***P_sp***	***N_sp***	***C_sp***	***Others***
HOMO	7.28%	48.53%	13.36%	12.99%	0.12%	9.01%	8.59%
LUMO	11.36%	0.30%	0.18%	4.70%	20.87%	61.53%	0.51%
S_1 state of the Cu_4H cluster							
	Cu_sp	***Cu_d***	***Cl_sp***	***P_sp***	***N_sp***	***C_sp***	***others***
HOMO	7.57%	45.85%	14.27%	13.61%	0.74%	8.71%	9.13%
LUMO	4.78%	1.20%	0.30%	5.54%	20.86%	65.93%	0.68%

Table S3. Standard Electrode Potentials.

Electric pair symbol	Electrode process	E^{θ}(V)
Zn^{2+}/Zn	$Zn^{2+}+2e^{-}=Zn$	-0.7626
Ni^{2+}/Ni	$Ni^{2+}+2e^{-}=Ni$	-0.257
Na^{+}/Na	$Na^{+}+e^{-}=Na$	-2.714
Mn^{2+}/Mn	$Mn^{2+}+2e^{-}=Mn$	-1.18
Ag^{+}/Ag	$Ag^{+}+e^{-}=Ag$	0.7991
Mg^{2+}/Mg	$Mg^{2+}+2e^{-}=Mg$	-2.356
Fe^{3+}/Fe	$Fe^{3+}+3e^{-}=Fe$	-0.037
Fe^{2+}/Fe	$Fe^{2+}+2e^{-}=Fe$	-0.44
Fe^{3+}/Fe^{2+}	$Fe^{3+}+e^{-}=Fe^{2+}$	0.771
Co^{2+}/Co	$Co^{2+}+2e^{-}=Co$	-0.277
Ca^{2+}/Ca	$Ca^{2+}+2e^{-}=Ca$	-2.868
Cu^{2+}/Cu^{+}	$Cu^{2+}+e^{-}=Cu^{+}$	0.159